

# Bose-Einstein condensation of five $\alpha$ clusters in $^{20}\text{Ne}$ and supersolidity

S. Ohkubo<sup>1\*</sup>, J. Takahashi<sup>2</sup> and Y. Yamanaka<sup>3</sup>

<sup>1\*</sup>Research Center for Nuclear Physics, Osaka University, Ibaraki, 567-0047, Japan.

<sup>2</sup>Faculty of Economics, Asia University, Tokyo, 180-0022, Japan.

<sup>3</sup>Institute of Condensed-Matter Science, Waseda University, Tokyo, 169-8555, Japan.

\*Corresponding author(s). E-mail(s): [ohkubo@rcnp.osaka-u.ac.jp](mailto:ohkubo@rcnp.osaka-u.ac.jp);

## Abstract

We show that the five  $\alpha$  cluster states recently observed in  $^{20}\text{Ne}$ , slightly above the five  $\alpha$  threshold energy, are Bose-Einstein condensates of five  $\alpha$  clusters. The states are described well using a superfluid cluster model, where the order parameter is defined. We suggest that the five  $\alpha$  states are fragmented. Theory predicts the emergence of a five  $\alpha$  rotational roton band characterized by a large moment of inertia. This band is formed through roton excitations of the five  $\alpha$  BEC vacuum and possesses dual properties of superfluidity and crystallinity, a property of supersolidity. The persistent existence of such a roton band is discussed and confirmed for the four  $\alpha$  condensate above the four  $\alpha$  threshold in  $^{16}\text{O}$  and the three  $\alpha$  condensate above the three  $\alpha$  threshold in  $^{12}\text{C}$ .

**Keywords:**  $\alpha$  condensation,  $^{20}\text{Ne}$ , roton excitation, supersolidity

## 1 Introduction

In analogy to BCS theory in nuclei [1–3] collective motions of superfluidity caused by  $\alpha$  cluster condensation have received attention within the framework of many-body theory over the last decades [4, 5]. Inspired by the observation of Bose-Einstein condensation (BEC) of trapped cold atoms [6], extensive theoretical [7–12] and experimental [13–19] studies have focused on the BEC of three  $\alpha$  clusters in the Hoyle state and excited states with a well-developed  $\alpha$  cluster structure above the  $\alpha$  threshold energy in  $^{12}\text{C}$ . Also the BEC of the four  $\alpha$  clusters in  $^{16}\text{O}$  above the four  $\alpha$  threshold has been studied theoretically [7, 20–23] and experimentally [24–30].

For the confirmation of the BEC of  $\alpha$  cluster structures, regardless of the number of  $\alpha$  clusters in the lowest 0s state ( $\sim 70\%$  for the Hoyle state in  $^{12}\text{C}$  [8] and 61% for the  $0^+$  state at 15.1 MeV in  $^{16}\text{O}$  [20]), it is essential to observe the Nambu-Goldstone (NG) mode due to global phase locking and the related collective motions of the BEC. The observation of typical phenomena such as superfluidity [3], roton excitations [31–36], quantum vortex [6], or the Josephson effect [37, 38] would definitively confirm the existence of BEC of  $\alpha$  cluster structures. A superfluid cluster model (SCM) based on effective field theory, in which the order parameter of BEC is defined and the NG mode operators originating in spontaneous symmetry breaking (SSB) of the global

phase are properly formulated [39], has successfully confirmed the BEC of  $\alpha$  cluster structure in  $^{12}\text{C}$  [11, 12] and  $^{16}\text{O}$  [21].

In He II, collective excitations involving a phonon of the NG mode and a roton [31–36] have been extensively investigated [40–47]. These excitations were confirmed experimentally in inelastic neutron scattering [48] and the rotation of He II [49]. In dipolar Bose-Einstein condensates of cold atoms [50–53], observations of roton excitations suggest the possibility of accessing a superfluid with order, a supersolid [54–56]. The existence of a supersolid in nature and the mechanisms behind its creation [57–60] have been long-standing questions since the discovery of He II [61, 62]. Notably, recent reports include the observation of a supersolid in optically trapped cold atoms [63–66] and the supersolidity of  $\alpha$  cluster structures at low excitation energies in nuclei [67, 68].

Recently Adachi et al. [69] observed three five  $\alpha$  cluster condensate candidate ( $0^+$ ) states in  $^{20}\text{Ne}$  at  $E_x=21.2, 21.8$  and  $23.6$  MeV in addition to the  $22.5$  MeV state observed by Swartz et al. [70]. A five  $\alpha$  cluster model calculation [71] yielded only two candidates  $0^+$  states. It is crucial to determine whether the observed four five  $\alpha$  states in  $^{20}\text{Ne}$  are indeed BEC states by confirming the NG mode and the collective motions associated with BEC. Also, understanding the BEC structure in  $^{20}\text{Ne}$  and the four  $\alpha$  (three  $\alpha$ ) BEC structure in  $^{16}\text{O}$  ( $^{12}\text{C}$ ), where the bands with the  $\alpha$  cluster structure are built on the NG mode  $0^+$  state, in a unified way is essential.

In this paper we show that the observed  $\alpha$  cluster states in  $^{20}\text{Ne}$  are BEC states by using the SCM and predict the emergence of a rotational band with a large moment of inertia. The band is shown to be caused by roton excitations of the five  $\alpha$  BEC vacuum and has a dual property of superfluidity and crystallinity, a property of a supersolid. The persistence of such a duality is discussed and confirmed for the bands with the four  $\alpha$  cluster condensate states in  $^{16}\text{O}$  and the three  $\alpha$  cluster condensate states in  $^{12}\text{C}$ .

## 2 Five $\alpha$ condensation in $^{20}\text{Ne}$

In the SCM [11, 39], the model Hamiltonian for a bosonic field  $\hat{\psi}(x)$  ( $x = (\mathbf{x}, t)$ ) representing the  $\alpha$

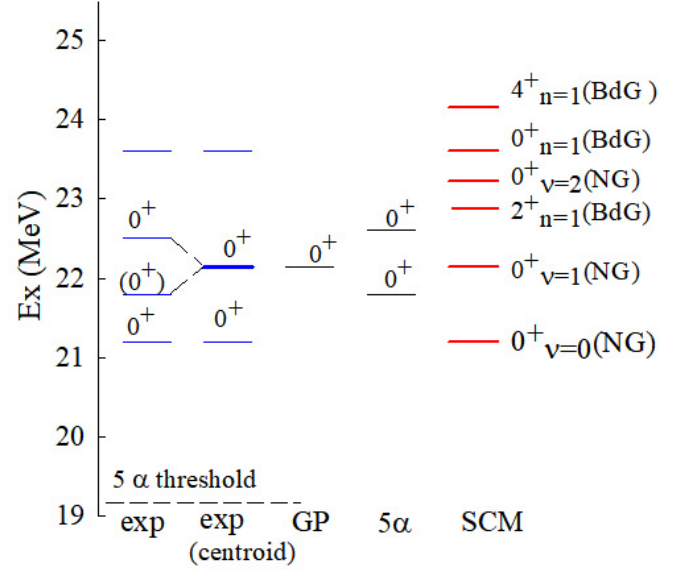


**Fig. 1** The experimental energy levels of the five  $\alpha$  condensate candidate states in  $^{20}\text{Ne}$  [69, 70] are compared with the calculations, the SCM, the Gross-Pitaevskii model (GP) [73], and the five  $\alpha$  cluster model ( $5\alpha$ ) [71]. Fragmentation is assumed for the two levels from the centroid indicated by the bold line.

cluster is given as follows:

$$\hat{H} = \int d^3x \hat{\psi}^\dagger(x) \left( -\frac{\nabla^2}{2m} + V_{\text{ex}}(\mathbf{x}) - \mu \right) \hat{\psi}(x) + \frac{1}{2} \int d^3x d^3x' \hat{\psi}^\dagger(x) \hat{\psi}^\dagger(x') U(|\mathbf{x} - \mathbf{x}'|) \hat{\psi}(x') \hat{\psi}(x). \quad (1)$$

The trap potential  $V_{\text{ex}}$  has  $V_{\text{ex}}(r) = m\Omega^2 r^2/2$ , and the  $\alpha$ - $\alpha$  interaction is given by  $U(|\mathbf{x} - \mathbf{x}'|) = V_r e^{-\mu_r^2 |\mathbf{x} - \mathbf{x}'|^2} - V_a e^{-\mu_a^2 |\mathbf{x} - \mathbf{x}'|^2}$  [72]. When BEC of  $\alpha$  clusters occurs, we decompose  $\hat{\psi}$  as  $\hat{\psi}(x) = \xi(r) + \hat{\varphi}(x)$ . The Gross-Pitaevskii (GP) equation determines the order parameter  $\xi(r)$  by  $\left\{ -\frac{\nabla^2}{2m} + V_{\text{ex}}(r) - \mu + V_H(r) \right\} \xi(r) = 0$  where  $V_H(r) = \int d^3x' U(|\mathbf{x} - \mathbf{x}'|) \xi^2(r')$  and  $\mu$  is the chemical potential.  $\xi$  is normalized with the condensed particle number  $N_0$  as  $\int d^3x |\xi(r)|^2 = N_0$ . The collective excitations on the condensate are described by the Bogoliubov-de Gennes (BdG) equation. The NG equation,  $\hat{H}_\nu^{QP} |\Psi_\nu\rangle = E_\nu |\Psi_\nu\rangle$  ( $\nu = 0, 1, \dots$ ) (see Refs. [11, 39] for

details), determines the NG mode  $0^+$  states. The excitation spectrum is obtained by solving these three coupled equations.

The two parameters  $\Omega$  and  $V_r$ , which control the size and stability of the trapped condensate, respectively, are determined as in Refs. [11, 12, 21]. The chemical potential is fixed by the input  $N_0=5$ . Assuming a condensation rate of 50%, considering  $\sim 60\%$  of the four  $\alpha$  condensate  $0^+$  state at 15.1 MeV in  $^{16}\text{O}$  [20, 21], we initially considered the lowest excited state at 21.2 MeV above the five  $\alpha$  threshold as the vacuum. However, although the SCM reproduces all the observed states, the resulting calculated rms radius  $\bar{r}$  of the 21.2 MeV  $0^+$  state (4.29 fm) is significantly smaller than the  $\bar{r}=5.62$  fm of the calculated four  $\alpha$  condensate  $0^+$  state at 15.1 MeV in  $^{16}\text{O}$  [21], rendering it physically unacceptable. This discrepancy suggests that at least one of the observed four states is fragmented.

In Fig. 1 the energy levels calculated with  $\Omega=1.06$  MeV/ $\hbar$  and  $V_r=505$  MeV are displayed. These calculations are based on taking the 21.2 MeV  $0^+$  state as the vacuum and assuming that the two states at 21.8 and 22.5 MeV are fragmented from the centroid. The resulting calculated vacuum radius  $\bar{r}=6.04$  fm is reasonable, comparable to the 5.5 fm in Ref. [73]. The calculation reproduces the experimental (centroid) data and locates the BdG  $2^+$  state at 22.9 MeV and  $4^+$  state at 24.2 MeV. The NG mode  $0^+$  states appear at 22.2 and 23.2 MeV. On the other hand, Refs. [71, 73] only calculated the  $0^+$  states, which are slightly higher than the experimental data.

In Fig. 2, it is surprising that a rotational band,  $K_{\text{rot}}$ , emerges on the NG mode  $0^+$  state. In the SCM, we assume no geometrical intrinsic configuration for the five  $\alpha$  clusters trapped in the spherical harmonic oscillator potential. Although it is not self-evident that the states form a rotational band from the viewpoint of field theory, the emergence of the  $K_{\text{rot}}$  band indicates that it has a common geometrically deformed intrinsic configuration for the five  $\alpha$  clusters. While the homogeneous He II system has a continuous spectrum, which consists of phonon excitations without angular momentum and roton ones with angular momentum, separated by the gap  $\Delta$  [31–36], the  $\alpha$  cluster system of the SCM is inhomogeneous due to the trap, resulting in discrete NG and BdG levels. We may identify the NG and BdG

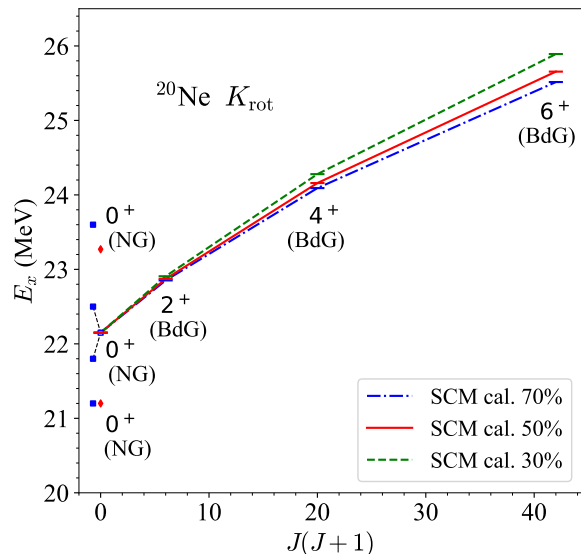


**Fig. 2** The calculated rotational band,  $K_{\text{rot}}$ , excited by rotons is built on the NG mode  $0^+$  of the five  $\alpha$  BEC in  $^{20}\text{Ne}$  for the condensation rates 30%, 50% and 70%. The experimental data are indicated by blue squares, and the lines are to guide the eye.

states in the SCM with the phonon and roton excitations in He II, respectively. Consequently, the states of the  $K_{\text{rot}}$  band correspond to roton excitations, and the energy of its head provides the gap  $\Delta$ . As indicated in Fig. 2, the emergence of the roton rotational band remains robust for different condensation rates of 30%, 50%, and 70%, with little change in the moment of inertia. Our calculations also confirm the appearance of the rotational roton band  $K_{\text{rot}}$  when the lowest two or three states are assumed to be fragmented from each centroid energy.

The rotational constant,  $k=\frac{\hbar^2}{2\mathcal{J}}$ , is estimated to be 67 keV from the band shown in Fig. 2, where

**Table 1**  $B(E2)$  values of the  $E2$  transitions in  $^{20}\text{Ne}$  calculated in the SCM for the condensation rates, (a) 30%, (b) 50% and (c) 70%, in units of  $e^2 \text{fm}^4$ .

Transition	(a)	(b)	(c)
$B(E2 : 2_{n=1}^+ (\text{BdG}) \rightarrow 0_{\nu=0}^+ (\text{NG}))$	440	786	1150
$B(E2 : 2_{n=1}^+ (\text{BdG}) \rightarrow 0_{\nu=1}^+ (\text{NG}))$	1690	2182	2541
$B(E2 : 4_{n=1}^+ (\text{BdG}) \rightarrow 2_{n=1}^+ (\text{BdG}))$	1283	1487	1628
$B(E2 : 6_{n=1}^+ (\text{BdG}) \rightarrow 4_{n=1}^+ (\text{BdG}))$	1761	2070	2301

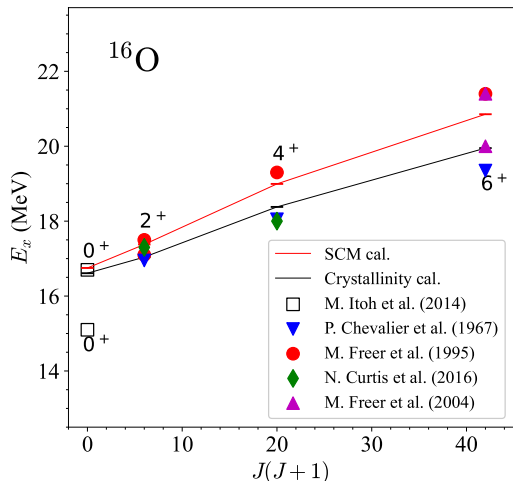


**Fig. 3** The four  $\alpha$  cluster rotational band  $K_{\text{rot}}$  in  $^{16}\text{O}$ . The theoretical calculations using the geometrical cluster model (crystallinity) [22] and the SCM [21] both reproduce the fragmented experimental states of the band from Ref. [26] and Refs. [24, 27, 29], respectively. The lines are to guide the eye.

$\mathcal{J}$  represents the moment of inertia. Comparatively,  $k=147$  keV for the  $K=0_1^-$  parity-doublet band starting at  $E_x=5.79$  MeV, while  $k=101$  keV for the  $K=0_4^+$  higher nodal band beginning at  $E_x \approx 8.78$  MeV with a very developed  $\alpha$  cluster structure in  $^{20}\text{Ne}$ . Notably, the  $\alpha$  cluster band  $K_{\text{rot}}$  in Fig. 2 has a significantly larger moment of inertia — about 3.0 times that of the  $K=0_1^+$  ground band in  $^{20}\text{Ne}$ . Accordingly, Table 1 predicts large  $B(E2)$  values for the roton band states, and similarly large values are obtained for the condensation rates of 30% and 70%. We note that the  $E2$  transition from the  $2_{n=1}^+$ (BdG) state to the band head  $0_{\nu=1}^+$ (NG) state is much stronger than that to the  $0_{\nu=0}^+$ (NG) state of the vacuum, reinforcing that the roton band is built on the first excited NG mode state.

The field theoretical excitations described above can be explained from the viewpoint of crystallinity, the geometrical configuration of the five  $\alpha$  clusters. Since the vacuum  $0^+$  state is spherical, the excited band states ( $0^+$ ,  $2^+$ ,  $4^+$  and  $6^+$ ) are attained by separating one  $\alpha$  cluster with the relative orbital angular momentum  $L=0, 2, 4$  and  $6$ , respectively. The band head  $0^+$  with  $L=0$  represents a higher nodal  $0^+$  state, in which the

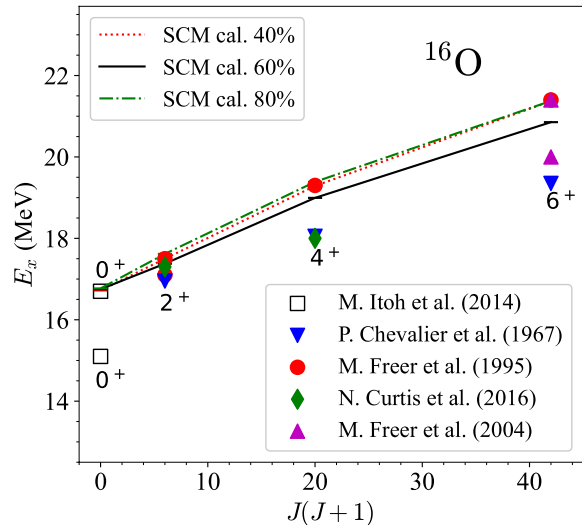


**Fig. 4** The emergence of the four  $\alpha$  rotational band  $K_{\text{rot}}$  in  $^{16}\text{O}$  in the SCM calculations [21] for the different condensation rates: 40, 60, and 80%. The lines are to guide the eye.

relative motion is excited to have one more node orthogonal to the vacuum. The  $K_{\text{rot}}$  band states form a rotational band with the configuration  $\alpha + (\text{core})$ , where the core consists of a four  $\alpha$  condensate of  $^{16}\text{O}$ . Thus, the  $K_{\text{rot}}$  band states exhibit not only superfluidity of roton excitations but also a deformed geometrical structure, a duality of superfluidity and crystallinity. A system with this duality is a supersolid, which has been long sought in He II [57–60]. A promising experimental approach to confirm BEC of the five  $\alpha$  clusters in  $^{20}\text{Ne}$  may involve observing the predicted rotational roton band due to roton excitations above the five  $\alpha$  threshold, which is highly desired.

### 3 Discussion

Since the rotational band  $K_{\text{rot}}$  has not yet been observed in  $^{20}\text{Ne}$ , it is important to know whether such a band exists in  $\alpha$  cluster nuclei where  $\alpha$  condensation has been intensively investigated theoretically and experimentally. Such candidate nuclei include  $^{12}\text{C}$  and  $^{16}\text{O}$ .

First we discuss  $^{16}\text{O}$ . In Fig. 3 the observed four  $\alpha$  cluster states [24–30], which are fragmented, are displayed. These states form a rotational band with a very large moment of inertia, have long been believed to have a geometrically linear chain of four  $\alpha$  clusters, as proposed in Ref. [24]. From the viewpoint of  $\alpha$  condensation, it was shown that the band can be better understood as having a geometrically  $\alpha+^{12}\text{C}(\text{g.s.}, 0_2^+)$  configuration, rather than the linear chain, in coupled channel cluster model calculations in Ref. [22].

On the other hand, the band states can also be well understood from the compelling viewpoint of a superfluid cluster model without assuming any geometrical configurations for four  $\alpha$  clusters [21]. As seen in Fig. 3, both pictures reproduce the experimental band almost equally. The two compelling properties of the band have not been understood in the literature consistently and in a unified way.

We suggest, as noticed in  $^{20}\text{Ne}$  theoretically, that the band states have a dual property of crystallinity and superfluidity. The band states with angular momentum are understood as roton excitations of the condensate vacuum, i.e., the rotational band states  $J = 2^+, 4^+$ , and  $6^+$  are understood to be caused by the roton excitations with angular momentum  $J = 2, 4$ , and  $6$ , from the condensate vacuum  $0^+$  state at 15.1 MeV. The band head  $0^+$  state is an NG state. To the authors' best knowledge, the roton excitations for finite systems like nuclei have never been noticed.

The geometrical cluster model's  $\alpha+^{12}\text{C}(0_2^+)$  configuration is consistently understood from the SCM calculation as follows: In the crystallinity picture, the  $0^+$  band head in Fig. 3 corresponds to a state where one of the four  $\alpha$  clusters in the vacuum is lifted to the next higher  $s$  orbit, resulting in a nonspherical  $\alpha+^{12}\text{C}(0_2^+)$  structure. The relative wave function has an additional node due to its orthogonality to the vacuum. Due to the SSB of rotational invariance, a rotational band with the  $\alpha+^{12}\text{C}(0_2^+)$  cluster structure emerges. In other words, the  $\alpha$  cluster rotates around the  $^{12}\text{C}(0_2^+)$  core with orbital angular momentum  $L=0, 2, 4$ , and  $6$ , corresponding to phonon (for  $L=0$ ) and roton (for  $L \neq 0$ ) excitations of the vacuum in the field theoretical picture. The rotational constant  $k=80$  keV calculated in the SCM agrees well with the estimated  $k=86$  keV from the crystallinity

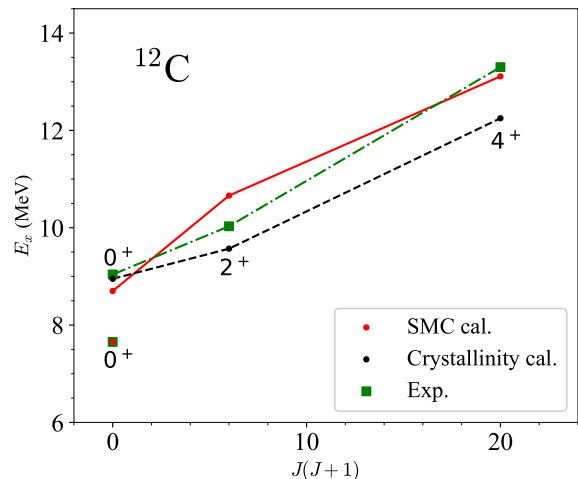


**Fig. 5** The three  $\alpha$  rotational band  $K_{\text{rot}}$  in  $^{12}\text{C}$ . The SCM [11] and the geometrical three  $\alpha$  cluster model (crystallinity) [76, 77] reproduce the experimental band from Refs. [15–18]. The lines are to guide the eye.

picture [22]. The fact that both pictures reproduce the experimental data of the four  $\alpha$  condensate in Fig. 3 indicates that the band exhibits the duality of superfluidity and crystallinity [68], characteristic of a supersolid. The large  $\mathcal{J}$  is the consequence of the roton excitations and it may serve as a fingerprint of supersolidity. This is understood intuitively because  $\mathcal{J}$  increases in  $J\hbar=\mathcal{J}\omega$  as the rotational frequency  $\omega$  approaches zero due to superfluidity.

In Fig. 4, one observes that the appearance of the roton band  $K_{\text{rot}}$  in  $^{16}\text{O}$  remains robust and almost unchanged for different condensation rates as for  $^{20}\text{Ne}$  shown in Fig. 2.

Next, we discuss  $^{12}\text{C}$ . Since it was demonstrated that the concept of the  $\alpha$  cluster condensate, with the dual properties of crystallinity and superfluidity, persists in the experimental data of  $^{16}\text{O}$ , it is expected that this concept may also persist in the three  $\alpha$  system of  $^{12}\text{C}$ , where most thorough study has been devoted both experimentally and theoretically.

As displayed in Fig. 5, the experimental states with a well-developed three  $\alpha$  cluster structure in  $^{12}\text{C} - 0_3^+$  (9.04 MeV) [17, 18],  $2_2^+$  (10.03 MeV) [15], and  $4_1^+$  (13.3 MeV) [16] – form a rotational band. In the crystallinity picture, the band head  $0_3^+$  is created by separating one  $\alpha$  cluster from the

spherical Hoyle state to a higher nodal state with  $L = 0$ , resulting in the  $\alpha+{}^8\text{Be}$  structure. In fact, the  $0_3^+$  state was shown to be the higher nodal state in geometrical three  $\alpha$  cluster model calculations using the orthogonality condition model (OCM) [74, 75]. More precise geometrical three  $\alpha$  cluster OCM calculations confirmed the  $\alpha+{}^8\text{Be}$  structure of the  $0_3^+$  state [76, 77]. The existence of the  $2^+$  and  $4^+$  states built on the  $0_3^+$  state, which was first predicted in Ref. [74, 75], was definitively confirmed in Ref. [76, 77]. The calculation based on the crystallinity picture reproduces the experimental rotational band as seen in Fig. 5 (dashed line).

On the other hand, the band is also well reproduced in the SCM calculation, as indicated by the solid line in Fig. 5. The calculation also predicts a  $6^+$  at 15.4 MeV in the roton band. In the SCM, the band head  $0_3^+$  is understood to be an NG mode state, while the  $2^+$ ,  $4^+$  and  $6^+$  band states result from roton excitations of the vacuum Hoyle  $0^+$  (7.65 MeV) state. The results in Fig. 5 are calculated with  $\Omega=1.80$  MeV/ $\hbar$ ,  $V_r=422$  MeV and  $N_0=3$ , as in Ref. [11]. We note that  $\alpha$  cluster model calculations based on the  $\alpha$  condensation picture of Ref. [9] with no order parameter and no particle number fluctuations do not reproduce the experimental rotational band, locating the  $2_2^+$  state lower than the band head  $0_3^+$ .

Thus, it is also found that the concept of duality of superfluidity and crystallinity, persists in the observed rotational band with a large moment of inertia, built just above the condensate vacuum, the Hoyle state. It is challenging to observe a roton band with supersolidity in other nuclei such as  ${}^{24}\text{Mg}$  and  ${}^{28}\text{Si}$ , which will serve as a unique fingerprint of BEC of the  $\alpha$  clusters.

## 4 Summary

To summarize, we have shown that the recently observed five  $\alpha$  cluster states above the five  $\alpha$  threshold in  ${}^{20}\text{Ne}$  are BEC states, using a superfluid cluster model. The emergence of a rotational band due to roton excitations, the roton band, is predicted in  ${}^{20}\text{Ne}$ .

The existence of the rotational roton bands with  $\alpha$  cluster structure of four  $\alpha$  cluster states in  ${}^{16}\text{O}$  and three  $\alpha$  cluster states in  ${}^{12}\text{C}$  is discussed and demonstrated in the available experimental data. The roton bands were shown to

exhibit the dual properties of superfluidity and crystallinity—a characteristic of a supersolid.

The observation of a roton band, characterized by a large moment of inertia, may serve as a fingerprint for Bose-Einstein condensation of  $\alpha$  clusters and supersolidity. It is highly desired to observe the predicted roton band states in  ${}^{20}\text{Ne}$  experimentally.

**Acknowledgements.** The authors thank the Yukawa Institute for Theoretical Physics at Kyoto University for the hospitality extended during a stay in March 2024.

## References

- [1] A. Bohr, B. R. Mottelson: *Nuclear Structure*, Vol. II, (Benjamin, Inc., New York, 1975).
- [2] P. Ring, P. Schuck, *The Nuclear Many-Body Problem* (Springer-Verlag, Berlin, 1980).
- [3] D. M. Brink, R. A. Broglia, *Nuclear Superfluidity: Pairing in Finite Systems* (Cambridge University Press, Cambridge, 2005).
- [4] J. Eichler, M. Yamamura, Nucl. Phys. A **182**, 33 (1972).
- [5] Y. K. Gambhir, P. Ring, P. Schuck, Phys. Rev. Lett. **51**, 1253 (1983).
- [6] E. A. Cornell, C. E. Wieman, Rev. Mod. Phys. **74**, 875 (2002).
- [7] A. Tohsaki, H. Horiuchi, P. Schuck, G. Röpke, Phys. Rev. Lett. **87**, 192501 (2001).
- [8] H. Matsumura, Y. Suzuki, Nucl. Phys. A **739**, 238 (2004).
- [9] Y. Funaki, Phys. Rev. C **92**, 021302(R) (2015).
- [10] Y. Funaki, Phys. Rev. C **94**, 024344 (2016).
- [11] Y. Nakamura, J. Takahashi, Y. Yamanaka, S. Ohkubo, Phys. Rev. C **94**, 014314 (2016); **98**, 049901(E) (2018).
- [12] R. Katsuragi, Y. Kazama, J. Takahashi, Y. Nakamura, Y. Yamanaka, S. Ohkubo, Phys. Rev. C **98**, 044303 (2018).

- [13] M. Freer et al., Phys. Rev. C **80**, 041303(R) (2009).
- [14] W. R. Zimmerman et al., Phys. Rev. C **84**, 027304 (2011).
- [15] W. R. Zimmerman et al., Phys. Rev. Lett. **110**, 152502 (2013).
- [16] M. Freer et al., Phys. Rev. C **83**, 034314 (2011).
- [17] M. Itoh et al., Nucl. Phys. A **738**, 268 (2004).
- [18] M. Itoh et al., Phys. Rev. C **84**, 054308 (2011).
- [19] M. Itoh et al., J. Phys. Conf. Ser. **436**, 012006 (2013).
- [20] Y. Funaki et al., Phys. Rev. Lett. **101**, 082502 (2008).
- [21] J. Takahashi, Y. Yamanaka, S. Ohkubo, Prog. Theor. Exp. Phys. **2020**, 093D03 (2020).
- [22] S. Ohkubo, Y. Hirabayashi, Phys. Lett. B **684**, 127 (2010).
- [23] Y. Funaki, Phys. Rev. C **97**, 021304(R) (2018).
- [24] P. Chevallier, F. Scheibling, G. Goldring, I. Plessner, M. W. Sachs, Phys. Rev. **160**, 827 (1967).
- [25] M. Freer et al., Phys. Rev. C **51**, 1682 (1995).
- [26] M. Freer et al., Phys. Rev. C **70**, 064311 (2004).
- [27] M. Freer, J. Phys. G **31**, S1795 (2005).
- [28] M. Itoh et al., J. Phys. Conf. Ser. **569**, 012009 (2014).
- [29] N. Curtis et al., Phys. Rev. C **94**, 034313 (2016).
- [30] M. Barbui et al., Phys. Rev. C **98**, 044601 (2018).
- [31] L. D. Landau, J. Phys. (USSR) **5**, 71 (1941).
- [32] L. D. Landau, J. Phys. (USSR) **11**, 91 (1947).
- [33] R. P. Feynman, Phys. Rev. **91**, 1291 (1953).
- [34] R. P. Feynman, Phys. Rev. **91**, 1301 (1953).
- [35] R. P. Feynman, Phys. Rev. **94**, 262 (1954).
- [36] R. P. Feynman, Rev. Mod. Phys. **29**, 205 (1957).
- [37] B. D. Josephson, Phys. Lett. **21**, 608 (1966).
- [38] R. A. Broglia et al., Phys. Rev. C **105**, L061602 (2022).
- [39] Y. Nakamura, J. Takahashi, Y. Yamanaka, Phys. Rev. A **89**, 013613 (2014).
- [40] A. Griffin, *Excitations in a Bose Condensed Fluid* (Cambridge Studies in Low Temperature Physics, Vol. 4), edited by A. M. Goldman, P. V. E. McClintock, M. Springford (Cambridge University Press, Cambridge, 1993).
- [41] H. R. Glyde, *Excitations in Liquid and Solid Helium* (Oxford Series on Neutron Scattering in Condensed Matter, Vol. 9), edited by S. W. Lovesey, E. W. J. Mitchell (Oxford University Press, Oxford, 1995).
- [42] R. A. Cowley, A. D. B. Woods, Can. J. Phys. Cond. Mat. **49**, 177 (1971).
- [43] A. D. B. Woods, R. A. Cowley, Rep. Prog. Phys. **36**, 1135 (1973).
- [44] K. H. Andersen et al., J. Phys. Cond. Mat. **6**, 821 (1994).
- [45] K. H. Andersen, W. G. Stirling, J. Phys. Cond. Mat. **6**, 5805 (1994).
- [46] M. R. Gibbs et al., J. Phys. Cond. Mat. **11**, 603 (1999).
- [47] A. A. Milner, V. Milner, Phys. Rev. Lett. **131**, 166001 (2023).
- [48] H. Palevsky et al., Phys. Rev. **108**, 1346 (1957).

- [49] W. F. Vinen, *Nature* **181**, 1524 (1958).
- [50] D. H. J. O'Dell, S. Giovanazzi, G. Kurizki, *Phys. Rev. Lett.* **90**, 110402 (2003).
- [51] L. Santos, G. V. Shlyapnikov, M. Lewenstein, *Phys. Rev. Lett.* **90**, 250403 (2003).
- [52] P. B. Blakie, D. Baillie, R. N. Bisset, *Phys. Rev. A* **86**, 021604(R) (2012).
- [53] R. N. Bisset, P. B. Blakie, *Phys. Rev. Lett.* **110**, 265302 (2013).
- [54] J-N. Schmidt et al., *Phys. Rev. Lett.* **126**, 193002 (2021).
- [55] L. Chomaz et al., *Nat. Phys.* **14**, 442 (2018).
- [56] D. Petter et al., *Phys. Rev. Lett.* **122**, 183401 (2019).
- [57] A. F. Andreev, I. M. Lifshitz, *Sov. Phys. JETP* **29**, 1107 (1969).
- [58] G. V. Chester, *Phys. Rev. A* **2**, 256 (1970).
- [59] A. J. Leggett, *Phys. Rev. Lett.* **25**, 1543 (1970).
- [60] H. Matsuda, T. Tsuneto, *Suppl. Prog. Theor. Phys.* **46**, 411 (1970).
- [61] P. Kapitza, *Nature* **141**, 74 (1938).
- [62] J. F. Allen, A. D. Misener, *Nature* **142**, 643 (1938).
- [63] L. Tanzi et al., *Phys. Rev. Lett.* **122**, 130405 (2019).
- [64] F. Böttcher et al., *Phys. Rev. X* **9**, 011051 (2019).
- [65] L. Chomaz et al., *Phys. Rev. X* **9**, 021012 (2019).
- [66] G. Biagioni et al., *Nature*, **629**, 773 (2024).
- [67] S. Ohkubo, J. Takahashi, Y. Yamanaka, *Prog. Theor. Exp. Phys.* **2020**, 041D01 (2020).
- [68] S. Ohkubo, *Phys. Rev. C* **106**, 034324 (2022).
- [69] S. Adachi et al., *Phys. Lett. B* **819**, 136411 (2021).
- [70] J. A. Swartz et al., *Phys. Rev. C* **91**, 034317 (2015).
- [71] B. Zhou et al., *Nat. Com.* **14**, 8206 (2023).
- [72] S. Ali, A. R. Bodmer, *Nucl. Phys. A* **80**, 99 (1966).
- [73] T. Yamada, P. Schuck, *Phys. Rev. C* **69**, 024309 (2004).
- [74] C. Kurokawa, K. Kato, *Phys. Rev. C* **71**, 021301(R) (2005).
- [75] C. Kurokawa, K. Kato, *Nucl. Phys. A* **792**, 87 (2007).
- [76] S. Ohtsubo, Y. Fukushima, M. Kamimura, E. Hiyama, *Prog. Theor. Exp. Phys.* **2013**, 073D02 (2013).
- [77] S. Ohtsubo, Y. Fukushima, M. Kamimura, E. Hiyama, *J. Phys. Conf. Ser.* **569**, 012070 (2014).